

ОБЪЕДИНЕННЫЙ
ИНСТИТУТ
ЯДЕРНЫХ
ИССЛЕДОВАНИЙ

Дубна

E1-2007-66

J. Fedorišin^{1,*}, S. Vokál^{1,2,**}

WAVELET ANALYSIS OF ANGULAR SPECTRA
OF RELATIVISTIC PARTICLES IN ^{208}Pb INDUCED
COLLISIONS WITH EMULSION NUCLEI AT 158A GeV/c

Submitted to «Czechoslovak Journal of Physics»

¹University of P. J. Šafárik, Košice, Slovakia

²Joint Institute for Nuclear Research, Dubna

*E-mail: fedorisi@kosice.upjs.sk

**E-mail: vokal@sunhe.jinr.ru

2007

to
hvb
21/4/06

INTRODUCTION

Collective effects are very helpful diagnostic tool to study the properties of nuclear matter which may undergo qualitative change when heated and compressed in ultrarelativistic heavy-nuclei collisions. While the evidence of directed or elliptic flow is well established and not disputed, some collective particle flows are deemed exotic and they are not widely accepted, mainly due to the lack of persuasive experimental material. The example of such a doubtful multi-particle correlation is the so-called ring-like structure which could be supposedly intercepted in the angular spectra of particles produced in high-energy nuclear collisions. The appearance of ring-like structures can be explained by the two competitive theories, though both of them involve the same physical mechanism.

The first one is the idea of Cherenkov gluons proposed in [1,2] as an intuitive analogue of Cherenkov electromagnetic radiation. The second theory introduces Mach shock waves appearing in the wake of supersonic particle when traversing nuclear medium [3]. The both processes trigger the production of coherent waves whose propagation is determined by the cone centered along the direction of initial particle. The cone is described by angle θ defined as:

$$\cos \theta = \frac{c_{\text{medium}}}{v}, \quad (1)$$

where v is a velocity of particle producing the waves and c_{medium} is either the speed of gluons or sound characteristic for the probed nuclear medium. Originally, both theories were developed to be applied to «ordinary» cold nuclear matter, but with the advent of ultrarelativistic heavy-ion physics they obtained a fresh boost and several theoretical and phenomenological works were published trying to describe some peculiarities in the SPS and mainly RHIC data in terms of Cherenkov gluons [4–8] or Mach cones [9–12] propagating either through the extremely heated nuclear matter or even through the deconfined partonic medium. The energy deposited in Cherenkov gluons or Mach shock waves could be eventually transformed to additional secondary particles, although an impact of hadronization to this process is not very clear. In favourite case, the original conical structure would be preserved in the form of ring-like structures in the angular spectra of produced particles. Of course, the ring-like structures are

expected to be formed in a plane perpendicular to the direction of triggering particle which can be either a parton or a hadron if it is looked upon as a bunch of partons.

Assuming that the direction of initial particle coincides with the direction of impinging beam, the plane perpendicular to the direction of particle will coincide with azimuthal plane.

Thus, the distributions of both the azimuthal and polar angles of secondary particles must be investigated simultaneously to observe the ring-like structures. If only relativistic particles are selected for analysis, it is advantageous to work with pseudorapidities η rather than with polar angles.

An occurrence of ring-like structure could be manifested by peaks or bumps in η distribution of secondary particles. In order to distinguish this type of multiparticle correlation from the so-called jet-like structures, the additional requirement of approximately uniform azimuthal distribution is imposed, though this uniformity may not be observed at all scales.

1. EXPERIMENT

The experimental data used in the presented analysis were acquired within the experiment EMU12 [13] (Collaboration EMU01). The stacks of NIKFI BR-2 nuclear photoemulsions were horizontally irradiated at CERN SPS accelerator by the beam of ^{208}Pb nuclei at $158A$ GeV/c momenta. The photoemulsion method allows one to reconstruct tracks of all charged particles as well as to determine their azimuthal angles ϕ and polar angles θ which are measured with respect to the beam direction. The velocities of charged particles are used to assort them to the three main groups:

- single-charge relativistic particles (usually denoted as s -particles) with $\beta > 0.7$ which include mostly pions with a small admixture of single-charge projectile fragments;
- multicharge projectile fragments with $\beta \approx 0.99$;
- target fragments with $\beta < 0.7$;

The experimental data set consists of 510 inelastic min-bias events. For the purpose of this analysis only the s -particles are taken into account since they consist mainly of particles created in the collisions and thus there is a chance they could include the particles resulting from the searched effects as well. Simultaneously, the multiplicities N_s of s -particles can be adopted as a criterion for the centrality of the collisions due to the dependence of multiplicities of s -particles on collision impact parameter which was verified, for instance, by

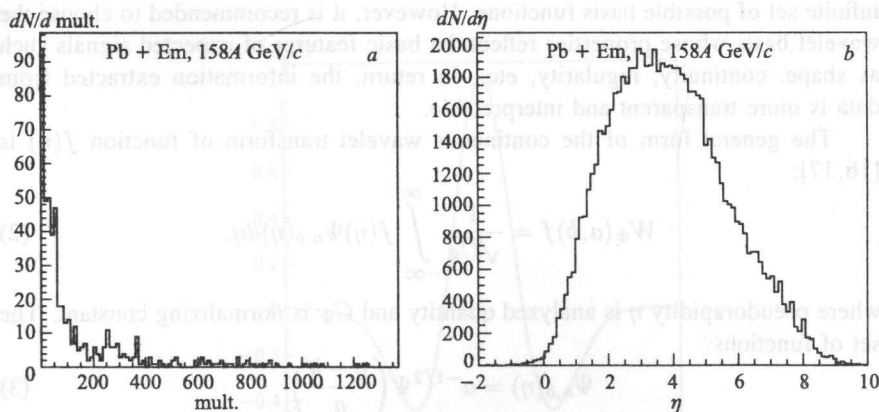


Fig. 1. Distributions of multiplicities (a) and pseudorapidities (b) of s -particles produced in Pb+Em interactions

the FRITIOF model [14, 15] simulations. The other important conclusion coming out of the simulations is that the target nuclei Ag(Br) are uniquely selected when $N_s > 350$, while under this limit value the studied sample may include also the collisions with the lighter nuclei such as C, N, O, H.

As can be easily seen in Fig. 1, a, the highest multiplicities of s -particles are above 1000.

Figure 1, b presents the pseudorapidity spectrum of all s -particles produced in the inelastic min-bias Pb+Em collisions.

2. METHOD

Our basic task is to analyze the pseudorapidity spectrum presented in Fig. 1, b, in order to find some conspicuous spikes or similar «irregularities» that could indicate the preferred emission polar angles in multiparticle production. An overabundance of secondary particles at some distinguished pseudorapidities is a necessary (though not sufficient) condition for the presence of ring-like structures. Due to rather vague or absent theoretical predictions we are barely able to estimate how many particles the ring-like structures might involve as well as their positions in the pseudorapidity spectrum. Therefore, it is inevitable to resort to data processing method capable to survey the η distribution at various scales in order to localize multiparticle correlations that may involve different numbers of particles.

The wavelet method fulfills the outlined requirements, providing practical mathematical apparatus to perform multiscale analysis. In addition, unlike Fourier analysis with only the two basis functions, the wavelet analysis offers theoretically

infinite set of possible basis functions. However, it is recommended to choose the wavelet basis whose properties reflect the basic features of expected signals such as shape, continuity, regularity, etc. In return, the information extracted from data is more transparent and interpretable.

The general form of the continuous wavelet transform of function $f(\eta)$ is [16,17]:

$$W_{\Psi}(a,b)f = \frac{1}{\sqrt{C_{\Psi}}} \int_{-\infty}^{\infty} f(\eta)\Psi_{a,b}(\eta)d\eta, \quad (2)$$

where pseudorapidity η is analyzed quantity and C_{Ψ} is normalizing constant. The set of functions

$$\Psi_{a,b}(\eta) = a^{-1/2}\Psi\left(\frac{\eta-b}{a}\right) \quad (3)$$

is shifted and/or dilated wavelets generated from the mother wavelet function $\Psi(\eta)$. They differ by translation parameter b and dilation parameter or scale a . The coefficients $W_{\Psi}(a,b)$ constitute the weights of wavelets $\Psi_{a,b}$ in spectrum $f(\eta)$, therefore the largest values of $W_{\Psi}(a,b)$ correspond to the prevailing scales a and pseudorapidities b . The whole process can be regarded as a mapping of spectrum $f(\eta)$ in scale-pseudorapidity space.

On the other hand, when applying Fourier expansion to a sample of pseudorapidities $\eta_1, \eta_2, \dots, \eta_N$ of s -particles in order to estimate a probability density $f(\eta)$, we converge to a sum of δ functions [18]:

$$f(\eta) = \frac{dn}{d\eta} = \frac{1}{N} \sum_{i=1}^N \delta(\eta - \eta_i), \quad (4)$$

which is a rather poor estimate of pseudorapidity density and provides no information on spectrum frequencies (scales). This significant drawback is overcome by applying the wavelet transform (2) to the function (4). The result is [19]:

$$W_{\Psi}(a,b)f = \frac{1}{N} \sum_{i=1}^N a^{-1/2}\Psi\left(\frac{\eta_i - b}{a}\right). \quad (5)$$

Wavelet pseudorapidity spectrum at some scale is thus the sum of wavelets representing individual particles. Wavelet coefficients $W_{\Psi}(a,b)$ reflect the probability to observe particle at some pseudorapidity b and scale a , which is again a slightly different reasoning why the wavelet coefficients are helpful to estimate prevailing scales and preferred pseudorapidities. The b -part of $W_{\Psi}(a,b)$ spectrum seen at various scales a cannot be interpreted directly as η probability density, though it is closely related to it. The reason is that all wavelet functions are normalized to 0, while a genuine probability density should be, as well known, normalized to 1.

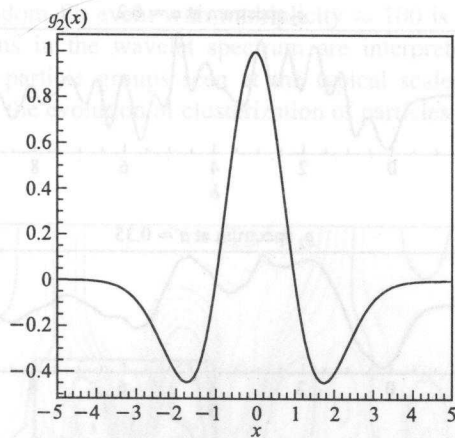


Fig. 2. The second derivative of Gaussian function, also known as Mexican hat

As for the choice of mother wavelet, after a few initial studies we decided to use the second derivative of Gaussian function (shown in Fig. 2) defined as

$$g_2 = (1 - x^2)e^{-x^2/2},$$

mainly because the Gaussian-like signals are assumed. The additional reason is that g_2 wavelet reaches a reasonable resolution in the scale and the pseudorapidity domains simultaneously.

3. WAVELET PSEUDORAPIDITY DISTRIBUTIONS

Event-by-event analysis is undoubtedly the most efficient way to study multiparticle correlations. Its great virtue is to observe unique features of individual events. Yet, as the very first test of the wavelet method, it may prove worthwhile to start with all the studied Pb events, although this approach is able to reveal only pronounced collective flows occurring systematically in many events.

Wavelet g_2 pseudorapidity spectra for all the s -particles at the three different scales a are presented in Fig. 3. They are the wavelet images of the distribution shown in Fig. 1, *b*.

As expected, the wavelet η spectrum at the large scales reveals only coarse features of the pseudorapidity distribution, whereas at the small scales an intricate fine structure is extracted.

The maximums in the spectra in Fig. 3 are associated with the preferred pseudorapidities of groups of secondary particles. There is a correlation between a scale and the size of particle groups seen at a corresponding scale, i. e., numerous

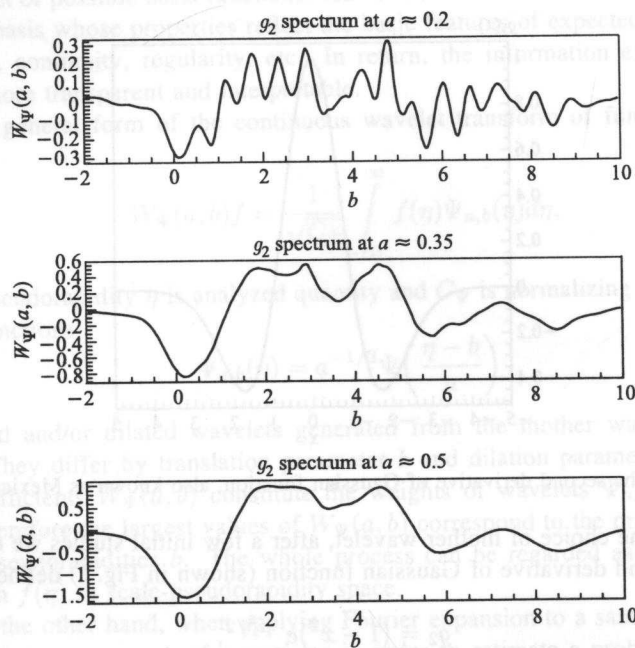


Fig. 3. Wavelet g_2 pseudorapidity spectra of all the studied Pb events seen at the three different scales a

particle groups occur more likely at large scales. The numbers of particles involved in separate groups can be estimated from the size of areas lying under the local maximums.

The particles can be roughly assorted to the three main groups: 1. the target fragmentation region at low pseudorapidities; 2. the projectile fragmentation region at high pseudorapidities; 3. the central region at medium pseudorapidities.

Basically, the similar structure of the wavelet pseudorapidity spectra was observed for the Au events at $11.6A$ GeV/c [20], where the analogous approach was first adopted. The differences are mainly in the size of central region which is more pronounced in the Pb data and in the behaviour at the smallest scales, where the Pb spectrum is obviously more structured and fluctuating, whereas the Au spectrum is relatively smooth. It implies that the Pb collisions are more tumultuous and unstable due to much larger collision energy.

There is no problem to create spectra like those in Fig. 3 for many scales a in the studied interval, i. e., to increase the density of scanning points along the scale axis. This will definitely produce more information about the behaviour of wavelet pseudorapidity spectrum in scale domain. In addition, such plots can be combined to create three-dimensional plot illustrating the dependence

of $W_\Psi(a, b)$ coefficients on pseudorapidity b and scale a simultaneously. The example for the random Pb event with multiplicity ≈ 100 is presented in Fig. 4. The local maximums in the wavelet spectrum are interpreted as the preferred pseudorapidities of particle groups seen at the typical scales. When travelling along the scale axis, the evolution of clusterization of particles can be investigated.

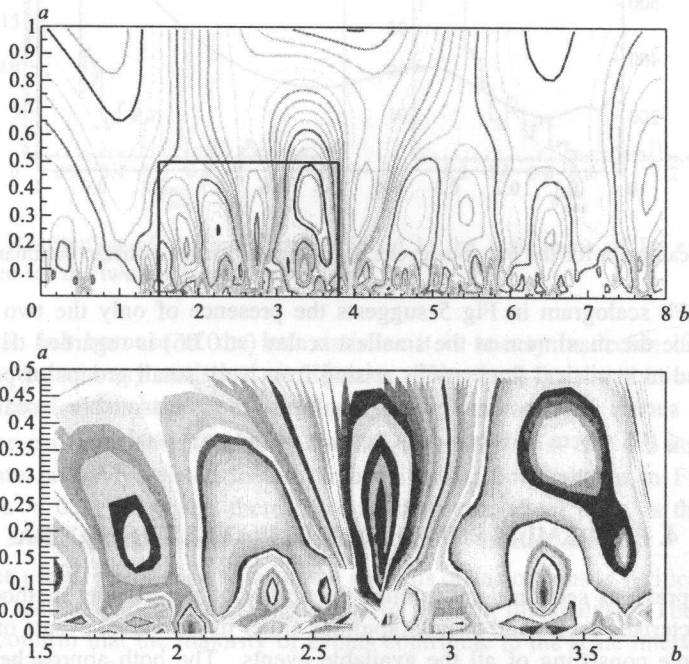


Fig. 4. Wavelet pseudorapidity spectrum of the random Pb event with multiplicity ≈ 100 . The lower picture is the rectangle area from the upper picture zoomed only to show better some interesting details

This leads to the explanation why the finest as well as the coarsest scales in the discussed plot are cut off. At too small scales only individual particles are recognized. On the contrary, at very large scales all particles lose identity in one huge bunch. Therefore, it does not make any sense to study clusterization effects in these two regions.

Figure 4 also suggests the interval of the most dominant scales since the maximums corresponding to groups of particles are found mainly in the scale range from 0.05 to 0.5. This is more explicit in the corresponding scalogram shown in Fig. 5. Scalogram (or scalegram) is defined as: $E_W(a) = \int W_\Psi(a, b)^2 db$. Its local maximums indicate prevailing scales.

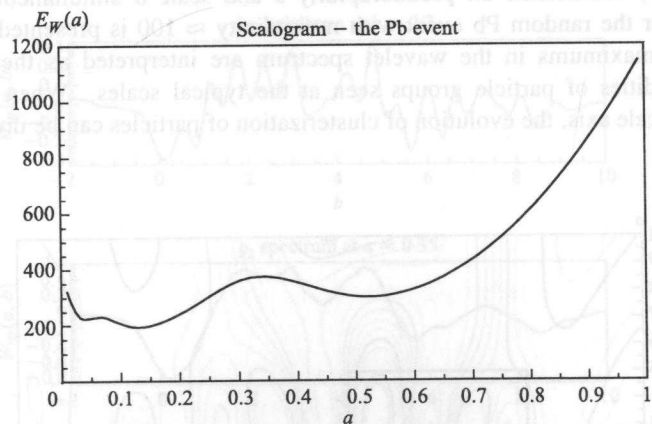


Fig. 5. Scalogram for the previous event. Its local maximums indicate dominant scales

The Pb scalogram in Fig. 5 suggests the presence of only the two relevant scales since the maximum at the smallest scales (< 0.05) is regarded trivial as it is ascribed to statistical fluctuations arising from very small groups of particles.

The survey of another events confirms the «reasonable» scale range $0.05 \leq a \leq 0.5$ where to focus our attention in the next analysis.

4. EXTREMUM POINTS IN THE WAVELET SPECTRA

The previous section demonstrates the ability of the wavelet method to find the characteristic scales and pseudorapidities either in individual events or in large data sample consisting of all the available events. The both approaches extract slightly different piece of information on multiparticle correlations which, when suitably combined, provide more complex and precise physical picture. The combination of the both concepts can be done by creating the spectra of relevant scales and pseudorapidities picked up from separate events. This procedure could answer the question whether event-by-event characteristic scales and pseudorapidities change randomly when going from one event to another, or they tend to appear repeatedly and systematically in many events.

Furthermore, this can be reasoned from the point of view of the pursued analysis. The ring-like structures are expected to occur at very close scales and probably only at a few distinguished (preferred) pseudorapidities in all the involved events which would be manifested by local maximums in the event-by-event wavelet pseudorapidity spectra $W_\Psi(a, b)$ of large sample of events.

Figure 6 presents the distribution of maximum points localized in the scalograms of all the Pb events. Some relevant scales are signaled at $0.05 \leq a \leq 0.1$

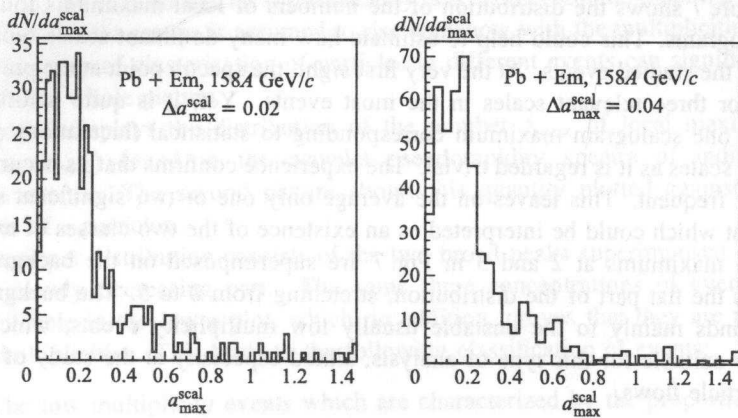


Fig. 6. Distribution of maximum points found in the scalograms of Pb events. It is presented for the two different binnings

$a \approx 0.2$, but because of the low statistics it is uneasy to decide if the signal candidates have any statistical significance. Therefore, the distributions in Fig. 6 are declared inconclusive.

One can notice the two other maximums emerging at $a \approx 0.5$ and $a \approx 0.6$. They are probably related to the large collective flows shown in Fig. 3 at the scales $a \approx 0.5$. However, there is no need to care about them as the searched effects are supposed to take place at considerably smaller scales.

The useful result ensuing from the analysis of scalograms is verification of the already recommended scale range where to perform the analysis. The spectra in Fig. 6 confirm that the majority of events contribute to the scale interval between 0.05 and 0.5 or 0.6.

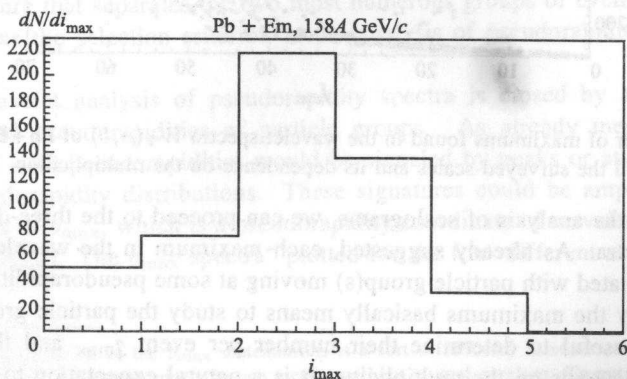


Fig. 7. Number of maximums found in the scalograms of Pb events

Figure 7 shows the distribution of the numbers of local maximums found in the scalograms. This could help to estimate how many dominant scales typically occur in the studied events. At the very first sight, the spectra point at the presence of two or three relevant scales in the most events. Yet, it is quite justified to subtract one scalogram maximum corresponding to statistical fluctuations at the smallest scales as it is regarded trivial. The experience confirms that its occurrence is rather frequent. This leaves on the average only one or two significant scales per event which could be interpreted as an existence of the two classes of events.

The maximums at 2 and 3 in Fig. 7 are superimposed on the background, which is the flat part of the distribution, stretching from 0 to 5. The background corresponds mainly to the unstable usually low multiplicity events, which are not very suitable for this type of analysis, aimed especially at the study of large multiparticle flows.

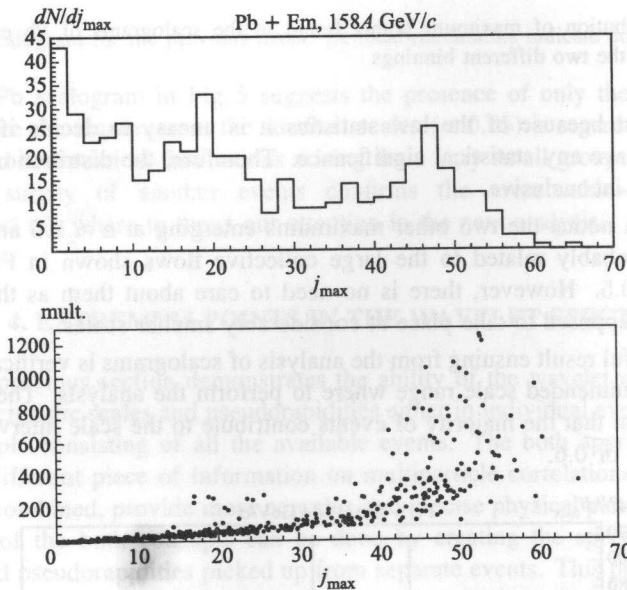


Fig. 8. Number of maximums found in the wavelet spectra $W_{\Psi}(a, b)$ of Pb+Em events in the range of all the surveyed scales and its dependence on the multiplicities

Closing the analysis of scalograms, we can proceed to the three-dimensional wavelet spectra. As already suggested, each maximum in the wavelet spectrum can be associated with particle group(s) moving at some pseudorapidity b . Therefore, to study the maximums basically means to study the particle groups. First, it could be useful to determine their number per event j_{\max} and then to find out how it depends on the multiplicity. It is a natural expectation to find in the events more small particle groups than the large ones, therefore the dependence

of dN/j_{\max} on j_{\max} should be approximately descending. On the other hand, the number of particle groups is assumed to rise somehow with the multiplicities. Of course, the way of clusterization of particles in different events can significantly influence the whole picture.

Figure 8 displays the distribution of the number j_{\max} of local maximums $W_{\Psi}(a_{\max}, b_{\max})$ found in the wavelet pseudorapidity spectra of individual Pb+Em events. The second picture shows this quantity plotted against multiplicities of s -particles.

The upper distribution consists of the two broad peaks superimposed on the smooth slowly decreasing part. The same three concentrations of events are clearly visible in the lower plot, which, in addition, proves that they are related to the multiplicities. This leads to the following classification of events:

- The low multiplicity events which are characterized by the proportionality between j_{\max} and the multiplicity. These events comprise mainly small particle clusters arising from statistical fluctuations.
- The stabilized and saturated high multiplicity events dominated by large collective particle flows. The term «saturated» is used because j_{\max} in these events does not depend on the multiplicities anymore and loosely converges to a single value. The last statement is only mere deduction that cannot be proved since the events with the multiplicities higher than 1300 are not represented in the available experimental ensemble.
- The small concentration of «peculiar» events lying roughly at mult. ≈ 200 and $j_{\max} \approx 20$. This anomaly was not present in the Au data [20].

The summary from Fig. 8 is an existence of the three classes of events in the data. The boundary between the first two discussed event classes is roughly estimated at the multiplicities about 200. As this boundary points at the change of event structure that separates the two most numerous groups of events, it is later introduced as the selection criterion in the analysis of pseudorapidity-azimuthal spectra.

The wavelet analysis of pseudorapidity spectra is closed by a search for the preferred pseudorapidities of particle groups. As already mentioned, the presence of such pseudorapidities would be signaled by peaks or at least bumps in the pseudorapidity distributions. These signatures could be amplified in the distributions of b_{\max} , which is a pseudorapidity coordinate of wavelet maximums $W_{\Psi}(a_{\max}, b_{\max})$. The b_{\max} spectra* plotted for the four different scale intervals

*The normalization of the b_{\max} distributions is a sort of arbitrary in some scale bands. This toll is paid to draw the spectra nicely in one picture without mutual overlaps. To put it another way, primarily the shapes of the distributions are important.

are presented in Fig. 9. The scale intervals are introduced to investigate how an occurrence of maximums $W_{\Psi}(a_{\max}, b_{\max})$ depends on scale.

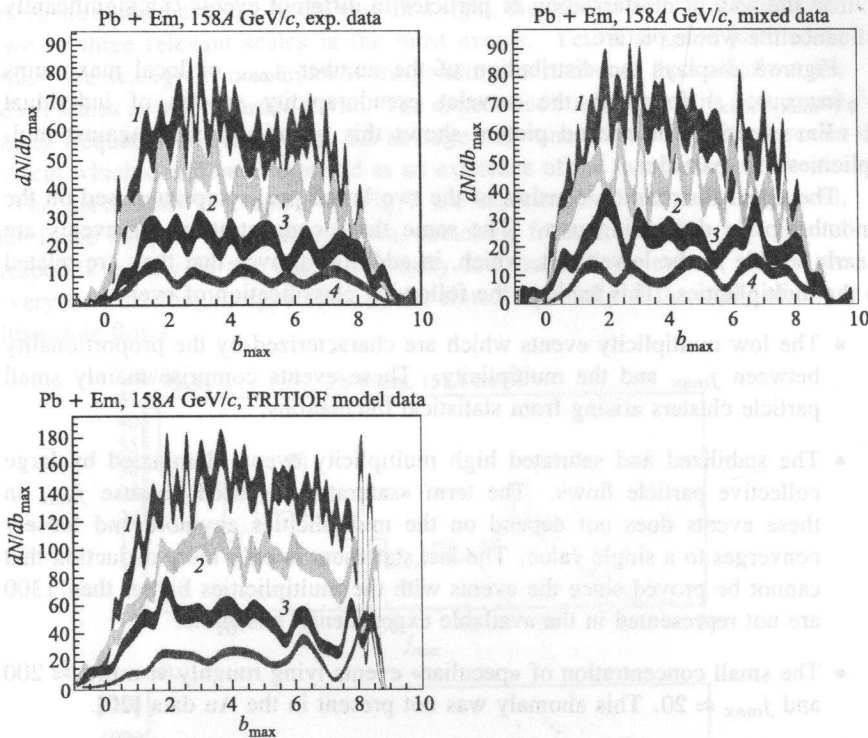


Fig. 9. The b_{\max} spectra of the experimental, mixed and FRITIOF model Pb+Em events seen in the four scale bands: 1) $0.05 < a_{\max} \leq 0.1$; 2) $0.1 < a_{\max} \leq 0.2$; 3) $0.2 < a_{\max} \leq 0.3$; 4) $0.3 < a_{\max} \leq 0.45$

Moreover, the analogous b_{\max} distributions are displayed for the FRITIOF model and the mixed data* to make some helpful comparisons.

The b_{\max} spectra in Fig. 9 are found irregular in all the examined scale bands. Local maximums which can be named irregularities are quite abundant, though not all of them are statistically relevant, which can be deduced from the outlined error corridors. Therefore, not all irregularities can be associated with multiparticle collective flows. However, some irregularities are persistent enough to reappear in the mixed data which is an argument for their non-incident occurrence in

*The mixed events are created to have some estimation of background. Therefore, only the tracks from experimental events with similar multiplicities are mixed to produce new events in order to maintain the structure of events.

the experimental data. More persuasive conclusions cannot be drawn since the statistical errors in the experimental plots are relatively large without a possibility to ever reduce them.

As for the FRITIOF model, it provides quite satisfactory description of the coarse features of the b_{\max} spectra except for some details at all the studied scales. The differences concern both the global shapes of the distributions and the shapes of the irregularities. Also, it seems some irregularities in the experimental data have no counterparts in the FRITIOF data, but this can be partly clarified by about two times larger statistics of the model events that results in smoother model distributions. The discrepancy at the end of the spectrum, though looking rather conspicuous at first sight, influences only the uninteresting tail of the distribution with not many particles involved (see Fig. 1, b) and does not prevent us from making sensible conclusions from the rest of the spectrum.

The essential issue if the irregularities revealed in the wavelet pseudorapidity spectra have something to do with the ring-like structures has not been solved yet. In order to answer this question it is inevitable to move forward to analysis of azimuthal distributions.

5. AZIMUTHAL DISTRIBUTIONS

The signatures for the preferred pseudorapidities of secondary particles emitted in the Pb+Em interactions found in the wavelet spectra do not constitute convincing evidence for the existence of ring-like structures. The competitive hypothesis elucidating an excess of particles at some distinguished pseudorapidities is an occurrence of «jet-like» structures. In our concept jet-like structure does not necessarily mean jet, but it is a more general term denoting group of particles correlated in both pseudorapidity and azimuth. There is no other way a to get rid of this ambiguity in the pseudorapidity distributions of secondary particles but to investigate concurrently their azimuthal distributions, especially their uniformity.

Approach to the azimuthal spectra is based on the previous analysis with one new substantial element brought in. Now the analogous event-by-event analysis is carried out separately in a few equal azimuthal sectors (see Fig. 10 for illustration). Wavelet pseudorapidity maximums $W_{\Psi}(a_{\max}, b_{\max})$ found at close scales and pseudorapidities but in different azimuthal sectors are combined to produce ring-like structure candidates. It is reasonable to assume that the ring-like structures should spread through a large number of azimuthal sectors, while jet-like structures will appear in only few, probably isolated, azimuthal sectors. Each ring-like structure candidate is thus characterized by a single variable n_{\max} denoting a number of involved azimuthal sectors. Primarily, n_{\max} is function of pseudorapidity and scale, but, in general, it may also depend on event multiplicity, centrality, etc.

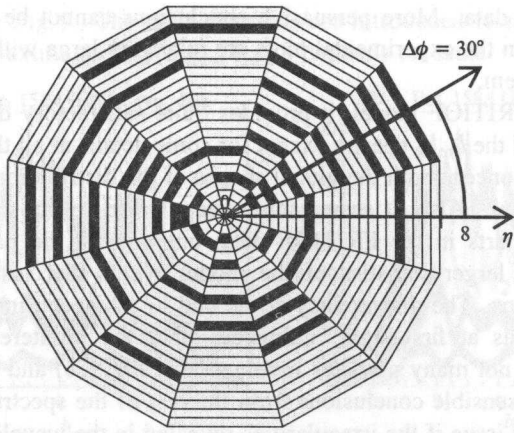


Fig. 10. An example of the target diagram for the random large multiplicity Pb + Em event (mult. > 1000) indicating the distribution of maximums $W_{\Psi}(a_{\max}, b_{\max})$ in azimuthal plane at scales $0.15 < a < 0.3$. The black slabs indicate η bins where maximums $W_{\Psi}(a_{\max}, b_{\max})$ are located

To conclude, a large value of n_{\max} observed at some pseudorapidity could suggest the presence of ring-like structure, while a small n_{\max} value is much likely just a result of randomly combined jet-like fluctuations either of statistical or non-statistical nature.

The ring-like structures seeking algorithm based on the outlined ideas is described elaborately in [20]. It is verified on the MC simulated data as well as the background and the mixed data samples in order to test and evaluate the method efficiency.

The choice of the total number of azimuthal sectors is based on the following considerations: a large total number of azimuthal sectors would mean a good azimuthal resolution but, on the other hand, a rather poor pseudorapidity resolution because the localization of wavelet maximums would be based on too small numbers of particles falling in each sector. On the contrary, to divide the total available range of azimuthal angles into very sizeable azimuthal sectors would entail precise determination of ring structures in pseudorapidity, but a ring structure detected in a low number of azimuthal sectors, though stretching over relatively large part of azimuth, would not be deemed very persuasive due to a weak azimuthal resolution. Of course, all the above variables depend on the multiplicities of events which are to be processed. It is not difficult to deduce the errors in azimuthal angle and pseudorapidity will be simultaneously diminished for the high multiplicity events. The reasonable boundary between the high and the low multiplicity events, which can be otherwise rather arbitrary, is offered in Fig. 8, where a sudden change in the behaviour of multiplicity vs j_{\max} distribution

is observed at the multiplicity about 200. Furthermore, the suggested value does not restrict the statistics of events left for analysis too much.

Finally, taking into account the previous reasoning, the total number of azimuthal sectors equaling 12 (or, 6) is chosen as an acceptable compromise achieving a satisfactory resolution of ring structures in both azimuth and pseudorapidity for the events with the multiplicities above 200. The alternative value of six azimuthal sectors is used as a double-check.

Normally, the spectra η vs n_{\max} in the different scale bands are examined to study the dependence of n_{\max} on pseudorapidity and scale as well. That could uncover if the ring structures candidates incline to appear casually or systematically at some characteristic pseudorapidities. In the experimental data (which is studied and discussed in the next section) these characteristic pseudorapidities should coincide with the previously found pseudorapidity irregularities presented in Fig. 9.

The Monte Carlo study is carried out only for the Au events for which the experimental conditions, and data ensembles were similar, and therefore the conclusions can be easily adjusted for the Pb data as well.

6. RESULTS

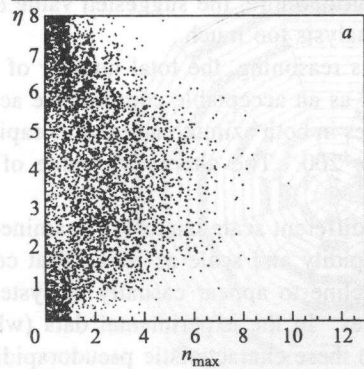
The Monte Carlo tests partly presented in [20] are found satisfactorily convincing of the capability of the method to detect the ring-like structures in the assumed scale range. After this verification we can eventually proceed to the last step which means an application of the ring structures finding method to the experimental data.

It is quite sufficient to present the η vs n_{\max} plots only for 12 azimuthal sectors since they are found fully compatible with the analogous plots when six azimuthal sectors are utilized. The another check consists in the comparison of the experimental η vs n_{\max} spectra with the corresponding distributions obtained from the FRITIOF model or the mixed data. If some promising candidates of ring-like structures are about to appear in the experimental plots, they should not have any counterparts in the model or the mixed data, where they are either not incorporated in the physical model or considerably suppressed by a mixing procedure (if they indeed occurred in the experimental data).

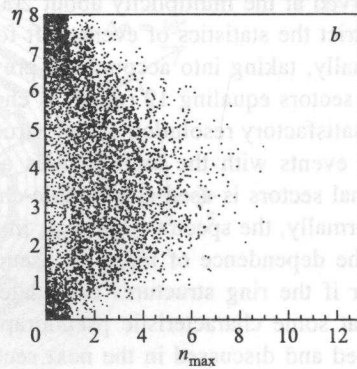
The η vs n_{\max} plots at the four different scale bands are displayed in Figs. 11–14. Each point in the η vs n_{\max} plots corresponds to a ring structure candidate spreading in n_{\max} azimuthal sectors.

We basically attempt to find some clusters of points jutting out of the compact background to the region of large n_{\max} where we believe to find ring-like structures. This should happen at only a few distinguished pseudorapidities η . In ideal case, the candidates for ring-like structures could get separated from background

Pb + Em, 158A GeV/c, experimental data



Pb + Em, 158A GeV/c, mixed data



Pb + Em, 158A GeV/c, FRITIOF model data

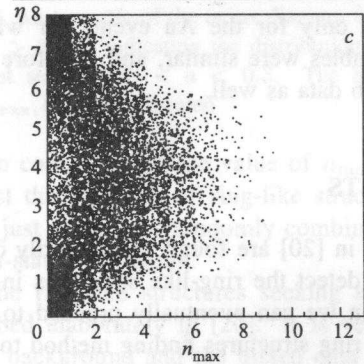
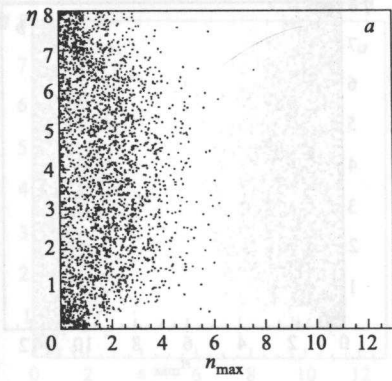


Fig. 11. Distribution of η vs n_{\max} in the scale band $0.05 < a_{\max} \leq 0.15$ ($a \approx 0.1$) for the Pb+Em experimental (a), mixed (b) and FRITIOF model (c) events with multiplicities above 200

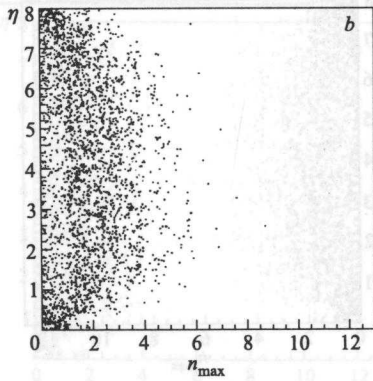
providing thus more convincing evidence of their existence. The background is interpreted as false ring structure candidates produced by random combinations of jet-like structures with close pseudorapidities. Due to the expectations it dominates the region of small n_{\max} .

The principal conclusion from the shown figures is the experimental η vs n_{\max} spectra that do not provide any proof for the searched effect since no suspicious behaviour that could be clarified by the presence of ring-like structures is intercepted. This statement is applicable for all the investigated scales. A few rare points deviating sporadically from the background in the experimental spectra do not constitute reliable evidence since the similar anomalies can be spotted in the model and the mixed data spectra as well. Furthermore, their occurrence on pseudorapidity axis seems erratic, without any trend to appear only at a few preferred pseudorapidities.

Pb + Em, 158A GeV/c, experimental data



Pb + Em, 158A GeV/c, mixed data



Pb + Em, 158A GeV/c, FRITIOF model data

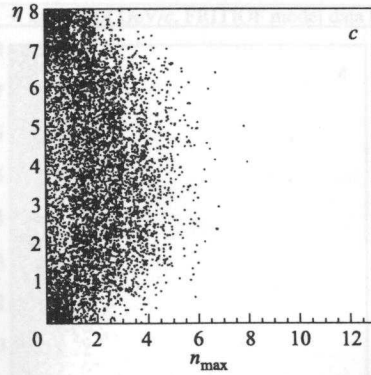


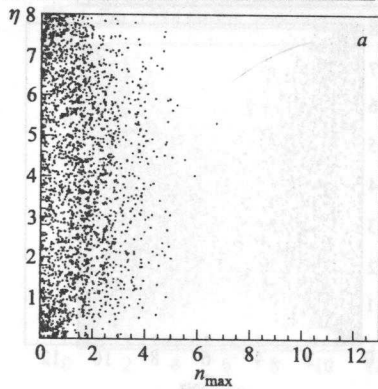
Fig. 12. Distribution of η vs n_{\max} in the scale band $0.15 < a_{\max} \leq 0.3$ ($a \approx 0.2$) for the Pb+Em experimental (a), mixed (b) and FRITIOF model (c) events with multiplicities above 200

A similar negative result was previously concluded for the Au+Em data published in [20].

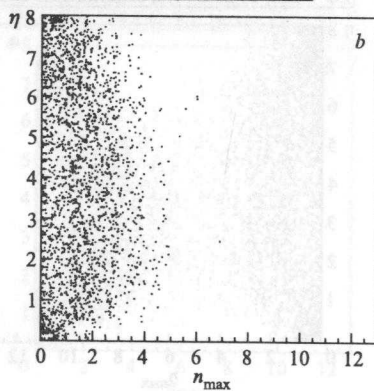
SUMMARY

- Pseudorapidity spectra of the relativistic secondary particles emitted in Pb+Em nuclear collisions at the SPS energies are analyzed by means of continuous wavelet transform.
- The local maximums referred to as irregularities are uncovered in the wavelet pseudorapidity distributions mainly in the scale range $a \leq 0.5$.

Pb + Em, 158A GeV/c, experimental data



Pb + Em, 158A GeV/c, mixed data



Pb + Em, 158A GeV/c, FRITIOF model data

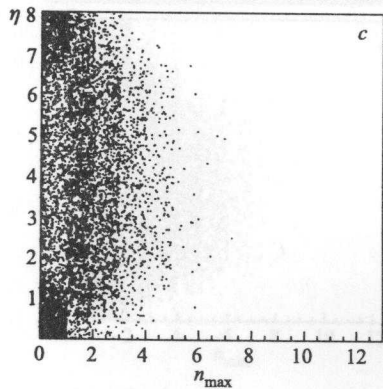


Fig. 13. Distribution of η vs n_{\max} in the scale band $0.2 < a_{\max} \leq 0.35$ ($a \approx 0.3$) for the Pb + Em experimental (a), mixed (b) and FRITIOF model (c) events with multiplicities above 200

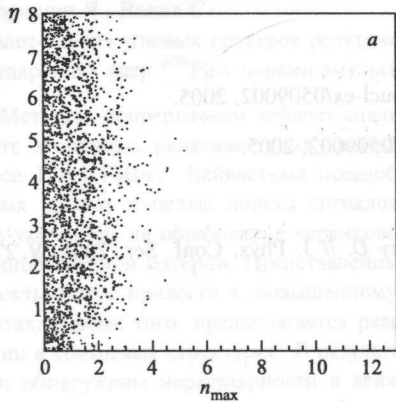
These irregularities indicate the preferred pseudorapidities of groups of emitted particles.

- The performed investigation of the azimuthal distributions of the above-mentioned pseudorapidity irregularities suggests they are not associated with the ring-like structures if these are defined as an excess of azimuthally uniformly distributed particles occurring at some characteristic pseudorapidities.

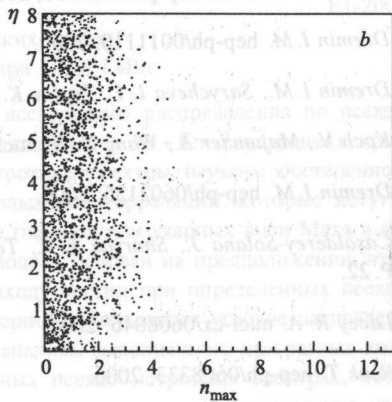
Acknowledgements. This work was supported by Slovak Research and Development Agency under the contract No. APVT-20-011704.

We also express our gratitude to V. V. Uzhinskii from LIT of JINR, Dubna,

Pb + Em, 158A GeV/c, experimental data



Pb + Em, 158A GeV/c, mixed data



Pb + Em, 158A GeV/c, FRITIOF model data

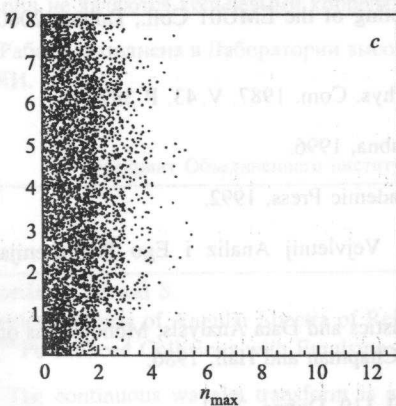


Fig. 14. Distribution of η vs n_{\max} in the scale band $0.3 < a_{\max} \leq 0.45$ ($a \approx 0.4$) for the Pb+Em experimental (a), mixed (b) and FRITIOF model (c) events with multiplicities above 200

for inspiration, collaboration and help with software support at the first stage of the presented experimental data analysis.

REFERENCES

1. Dremin I. M. // Pisma v ZhETF. 1979. V. 30. P. 152.
2. Dremin I. M. // Yad. Fiz. 1981. V. 33. P. 1357.
3. Glassgold A. E., Heckrotte W., Watson K. M. // Ann. Phys. 1959. V. 6. P. 1.

4. *Dremin I. M. et al.* hep-ph/0007060, 2000.
5. *Dremin I. M.* hep-ph/0011110, 2000.
6. *Dremin I. M., Sarycheva L. I., Teplov K. Y.* nucl-ex/0509002, 2005.
7. *Koch V., Majumder A., Wang X.-N.* nucl-th/0509002, 2005.
8. *Dremin I. M.* hep-ph/0602135, 2006.
9. *Casalderey-Solana J., Shuryak E. V., Teaney D.* // J. Phys. Conf. Ser. 2005. V. 27. P. 22.
10. *Lacey R. A.* nucl-ex/0608046, 2006.
11. *Renk T.* hep-ph/0608333, 2006.
12. *Renk T., Ruppert J.* // Phys. Rev. C. 2006. V. 73. P. 011901.
13. *Gaitinov A. et al.* // Proc. of the XVII Meeting of the EMU01 Coll., Dubna, 2000. P. 143.
14. *Nilsson-Almqvist B., Stenlund E.* // Comp. Phys. Com. 1987. V. 43. P. 387.
15. *Uzhinskii V.* // JINR Preprint E2-96-192. Dubna, 1996.
16. *Chui C. K.* An Introduction to Wavelets, Academic Press, 1992.
17. *Koronovskij A., Khranov A.* Nepreryvnyj Vejvletnij Analiz i Ego Prilozhenija. Moskva: Fizmatlit, 2003.
18. *Silberman B. W.* Density Estimation for Statistics and Data Analysis, Monographs on Statistics and Applied Probability. London: Chapman and Hall, 1986.
19. *Uzhinskii V. et al.* // JINR Commun. P1-2001-119. Dubna, 2001.
20. *Fedorišin J., Vokál S.* // JINR Preprint E1-2007-4. Dubna, 2007.

Received on April 26, 2007.

Федоришин Я., Вокал С.

E1-2007-66

Вейвлет-анализ угловых спектров релятивистских частиц
в соударениях ядер ^{208}Pb с ядрами эмульсии при 158A ГэВ/с

Методом непрерывного вейвлет-анализа исследованы распределения по псевдобыстроте вторичных релятивистских частиц, рожденных в $\text{Pb} + \text{Em}$ соударениях при импульсе 158A ГэВ/с . Вейвлетные псевдобыстротные спектры изучены постепенно при разных шкалах с целью поиска сигналов кольцевых корреляций, которые могут служить указанием на образование черенковских глюонов или ударных волн Маха в возбужденной ядерной материи. Представленный подход основан на предположении, что эти эффекты могут привести к повышенному выходу частиц при определенных псевдобыстротах. Кроме того, предполагается равномерное азимутальное угловое распределение частиц в кольцевых структурах. В результате анализа, выполненного при разных шкалах, были обнаружены нерегулярности в вейвлетных псевдобыстротных спектрах, которые нами интерпретируются как псевдобыстроты приоритетного испускания групп частиц. Исследование равномерности азимутальной структуры этих нерегулярностей показало, что они не являются кольцевыми корреляциями.

Работа выполнена в Лаборатории высоких энергий им. В. И. Векслера и А. М. Балдина ОИЯИ.

Препринт Объединенного института ядерных исследований. Дубна, 2007

Fedorišin J., Vokál S.

E1-2007-66

Wavelet Analysis of Angular Spectra of Relativistic Particles
in ^{208}Pb Induced Collisions with Emulsion Nuclei at 158A GeV/c

The continuous wavelet transform is applied to the pseudorapidity spectra of relativistic secondary particles created in $\text{Pb} + \text{Em}$ nuclear collisions at 158A GeV/c . The wavelet pseudorapidity spectra are subsequently surveyed at different scales to look for signs of ring-like correlations whose presence could be explained either via the production of Cherenkov gluons or the propagation of Mach shock waves in excited nuclear medium. The presented approach is established on the basic prerequisite that the both effects would lead to excess of particles at certain typical pseudorapidities. Furthermore, the particles contributing to the ring-like structures are expected to have uniform azimuthal distributions. The multiscale analysis of the wavelet pseudorapidity spectra reveals the irregularities which are interpreted as the favoured pseudorapidities of groups of produced particles. A uniformity of the azimuthal structure of the disclosed pseudorapidity irregularities is examined, eventually leading to the conclusion that the irregularities are not related to correlations of a ring-like nature.

The investigation has been performed at the Veksler and Baldin Laboratory of High Energies, JINR.

Preprint of the Joint Institute for Nuclear Research. Dubna, 2007